True amplitude migration using common-shot one-way wavefield extrapolation

YU ZHANG[1], JAMES SUN[1], SAMUEL H. GRAY[2], CARL NOTFORS[3],
NORMAN BLEISTEIN[4] and GUANQUAN ZHANG[5]
[1]*Veritas DGC Inc., Houston, USA* , [2]*Veritas DGC Inc., Calgary, Canada,* [3]*Veritas DGC Inc., Singapore,*
[4]*Colorado School of Mines, USA,* [5]*Chinese Academy of Sciences, Beijing, China*

Summary We analyze the amplitudes produced by shot-record migration using one-way wavefield extrapolation in a $v(z)$ medium. By comparing these amplitudes with those produced by true-amplitude Kirchhoff migration, we identify the amplitude and phase errors that come from a standard implementation of migration by one-way wavefield extrapolation. Next, we present a new formulation of shot-record migration that maintains its high fidelity in imaging complex structures and has correct dynamic behavior for a $v(z)$ velocity. This formulation requires that we modify, in a straightforward way, the surface data for wavefield that is being downward continued.

Introduction Until recently, Kirchhoff migration has been used for most 3-D prestack migrations, primarily because of its versatility and efficiency. The demands of imaging increasingly complex geological structures, however, have spurred a demand for increased imaging fidelity. This has led to the growing popularity of imaging methods that handle more than the single arrival that Kirchhoff migration is capable of handling conveniently. Such methods include finite-difference migration, which allows for an unlimited number of arrivals. In this paper, we concentrate on one-way wavefield extrapolation, paying particular attention to its amplitude and phase behavior.

The standard formulation of finite-difference migration (Claerbout, 1985) consists of two parts. The first part is the downward continuation of the wavefields from the source and receiver locations using a split "wave equation." The second part is the application of an imaging condition, namely the division of the downward continued receiver wavefield by the downward continued source wavefield at each image point. Unfortunately, the one-way "wave equations" used in the downward continuation are not equivalent to the acoustic wave equation whose behavior they are designed to mimic. This lack of equivalence leads to a migrated wavefield that lacks correct amplitude and phase behavior, even though it is kinematically correct. By expressing the downward continued wavefields asymptotically, we are able to compare the imaged wavefield with the reflection coefficient of true amplitude Kirchhoff migration. This comparison leads to a corrected equation for the upgoing and downgoing wavefields. When these corrections are applied, the migration produces images whose amplitudes and phases agree with true-amplitude Kirchhoff migration.

Theory We begin with a layered velocity ($v(z)$) earth and 3D common-shot migration. Given an acoustic wave-field p with source excitation at $\vec{x}_s = (x_s, y_s, 0)$ and $t = 0$,

$$\left(\frac{1}{v^2} \frac{\partial^2}{\partial t^2} - \frac{\partial^2}{\partial z^2} - \frac{\partial^2}{\partial x^2} - \frac{\partial^2}{\partial y^2} \right) p(x, y, z; t) = \delta(\vec{x} - \vec{x}_s)\delta(t), \tag{1}$$

we record the surface data Q:

$$p(x_r, y_r, z = 0; t) = Q(x_r, y_r; t). \tag{2}$$

According to Bleistein et al.'s (2001) work on inversion, the true-amplitude common shot Kirchhoff inversion formula is (Zhang, et al., 2000)

$$R(x, y, z) \sim \iiint i\omega \frac{\sqrt{\cos\alpha_{s0}\cos\alpha_{r0}}}{v_0}\sqrt{\frac{\psi_s\sigma_s}{\psi_r\sigma_r}}e^{i\omega(\tau_s+\tau_r)}\hat{Q}(x_r, y_r; \omega)dx_r dy_r d\omega, \tag{3}$$

where ψ and σ are in-plane and out-of-plane geometrical spreading terms and α_{s0} and α_{r0} are surface angles at shot and receivers, respectively (see Figure 1); hat denotes temporal Fourier transform.

For conventional common-shot migration, we downward continue both shot and receiver wavefields, D and U, which we assume to satisfy the following equations (Claerbout, 1985)

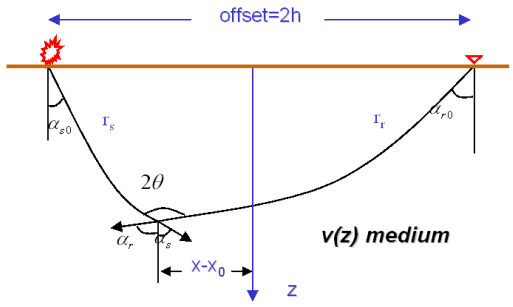

Figure 1: Ray paths in a $v(z)$ medium

$$\begin{cases}\left(\dfrac{\partial}{\partial z}+\Lambda\right)D(x, y, z; t)=0,\\ D(x, y, z=0; t)=\delta(\vec{x}-\vec{x}_s)\delta(t),\end{cases} \tag{4}$$

and

$$\begin{cases}\left(\dfrac{\partial}{\partial z}-\Lambda\right)U(x, y, z; t)=0,\\ U(x, y, z=0; t)=Q(x, y; t).\end{cases} \tag{5}$$

Here Λ is the square-root operator. To produce the image, we use the imaging condition

$$R(x, y, z)=\int\frac{\hat{U}(x, y, z; \omega)}{\hat{D}(x, y, z; \omega)}d\omega. \tag{6}$$

For a $v(z)$ medium, Zhang et al. (2001a) give an asymptotic expression for the one-way wave fields:

$$\hat{D}(x, y, z; \omega) \sim \frac{i\omega}{2\pi}\sqrt{\frac{\cos\alpha_s}{\psi_s\sigma_s}}e^{-i\omega\tau_s} \tag{7}$$

and

$$\hat{U}(x, y, z; \omega) \sim \iint\frac{i\omega}{2\pi}\sqrt{\frac{\cos\alpha_r}{\psi_r\sigma_r}}e^{i\omega\tau_r}\hat{Q}(x_r, y_r; \omega)dx_r dy_r. \tag{8}$$

Substituting (7) and (8) into (6), we obtain

$$R(x, y, z) \sim \iiint\sqrt{\frac{\cos\alpha_r\psi_s\sigma_s}{\cos\alpha_s\psi_r\sigma_r}}e^{i\omega(\tau_s+\tau_r)}\hat{Q}(x_r, y_r; \omega)dx_r dy_r d\omega. \tag{9}$$

Comparing (9) with (3), we conclude that the algorithm (4-6) cannot provide a true amplitude image; even the phase term $i\omega$ is missing from (9).

In Zhang et al. (2001b), we give a remedy to correct the amplitude for constant velocity, but an additional correction term needs to be applied for a $v(z)$ medium. Here we formulate the following modified phase-shift migration algorithm which gives the true amplitude common-shot migration result for $v(z)$ velocity. Its generalization to a completely heterogeneous $v(x, y, z)$ acoustic medium will be addressed in a separate paper.

Let $\tilde{p}(k_x, k_y; \omega)$ denote the spatial-temporal Fourier transform of the function $p(x, y; t)$. Instead of solving D and U, we propose to solve for pressure fields p_D and p_U, which satisfy the following equations (Zhang, 1993) and boundary conditions

$$\begin{cases} \left(\dfrac{\partial}{\partial z} + \lambda - \gamma\right)\tilde{p}_D(k_x, k_y, z; \omega) = 0, \\ \tilde{p}_D(k_x, k_y, z = 0; \omega) = \dfrac{1}{2\lambda} e^{i(k_x x_s + k_y y_s)}, \end{cases} \tag{10}$$

and

$$\begin{cases} \left(\dfrac{\partial}{\partial z} - \lambda - \gamma\right)\tilde{p}_U(k_x, k_y, z; \omega) = 0, \\ \tilde{p}_U(k_x, k_y, z = 0; \omega) = \tilde{Q}(k_x, k_y; \omega), \end{cases} \tag{11}$$

where

$$\lambda = i\frac{\omega}{v}\sqrt{1 - v^2\frac{k_x^2 + k_y^2}{\omega^2}} \qquad \text{and} \qquad \gamma = \frac{v_z}{2v}\frac{\omega^2}{\omega^2 - v^2(k_x^2 + k_y^2)}.$$

Also, we modify the imaging condition (6) to be the quotient of the wave fields p_D and p_U:

$$R(x, y, z) = \int \frac{\hat{p}_U(x, y, z; \omega)}{\hat{p}_D(x, y, z; \omega)} d\omega. \tag{12}$$

It can be proved that equations (10) and (11), together with imaging condition (12), give the same true amplitude result as (3) in the sense of high frequency approximation.

Numerical tests Figure 2 (left) shows the 3-D migrated impulse responses along the center inline from a trace with three 7.5Hz Ricker wavelets at depth 1000m, 2000m and 3000m, respectively. The source is at crossline 121 and receiver at crossline 141; trace spacing is 50m in both inline and crossline directions. The medium velocity is 2000m/s. Unlike the kinematic behavior, the amplitudes of the impulse responses are asymmetric, with a bias on the receiver side. The peak amplitudes along the impulse responses are in good agreement with the theoretical prediction shown in Figure 2 (right).

Figure 3 shows a 2-D true amplitude migration result from a single shot over four flat reflectors from density contrasts in a medium with velocity $v(z) = 2000 + 0.3z$. The input data (top) is generated by applying geometrical spreading to equal-amplitude Ricker wavelets with analytical traveltime. The bottom left is the migrated shot record. The peak amplitudes along the four migrated reflectors are shown in bottom right. Aside from the edge effects and small jitters caused by interference with wraparound artifacts, the $v(z)$ true amplitude common shot migration recovers the reflectivity accurately.

Conclusions Migrations based on one-way wavefield extrapolation offer the potential of greater structural imaging quality than single-arrival Kirchhoff migration. However, the standard formulation of such migrations, e.g. finite-difference migration, produce incorrect migrated amplitudes. By comparing these amplitudes with those produced by true-amplitude Kirchhoff migration, we have, in effect, calibrated these migration methods, correcting their amplitude and phase behavior.

References

Bleistein, N., Cohen, J. K., and Stockwell, J. W., 2001, Mathematics of multidimensional seismic inversion: Springer.

Claerbout, J., 1985, Imaging the earth's interior: Blackwell Scientific Publication, Inc.

Zhang, G., 1993, System of Coupled Equations for Up-going and Down-going waves, Acta Math. Appl. Sinica, **16:2**, 251-263.

Zhang, Y., Gray, S., and Young, J., 2000, Exact and approximate weights for Kirchhoff migration: 70th Ann. Mtg., Soc. Expl. Geophys., Expanded Abstracts, 1036-1039.

Zhang, Y., Gray, S. and Young, J., 2001a, True-amplitude Common-offset, Common-azimuth *v(z)* Migration, Journal of Seismic Exploration (accepted).

Zhang, Y., Sun, J., Gray, S., Notfors, C. and Bleistein, N., 2001b, Towards Accurate Amplitudes for One-way Wavefield Extrapolation of 3-D Common Shot Records, 71st Ann. Mtg., Soc. Expl. Geophys (Workshop).

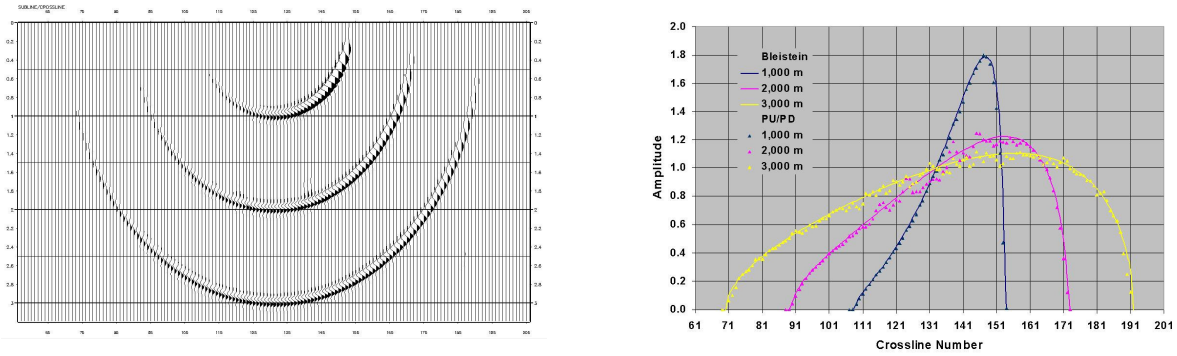

Figure 2: Left: 3-D phase-shift migrated impulse responses along the center inline. The shot is at crossline 121 and receiver at crossline 141. Right: Amplitudes of the 3-D migrated impulse responses.

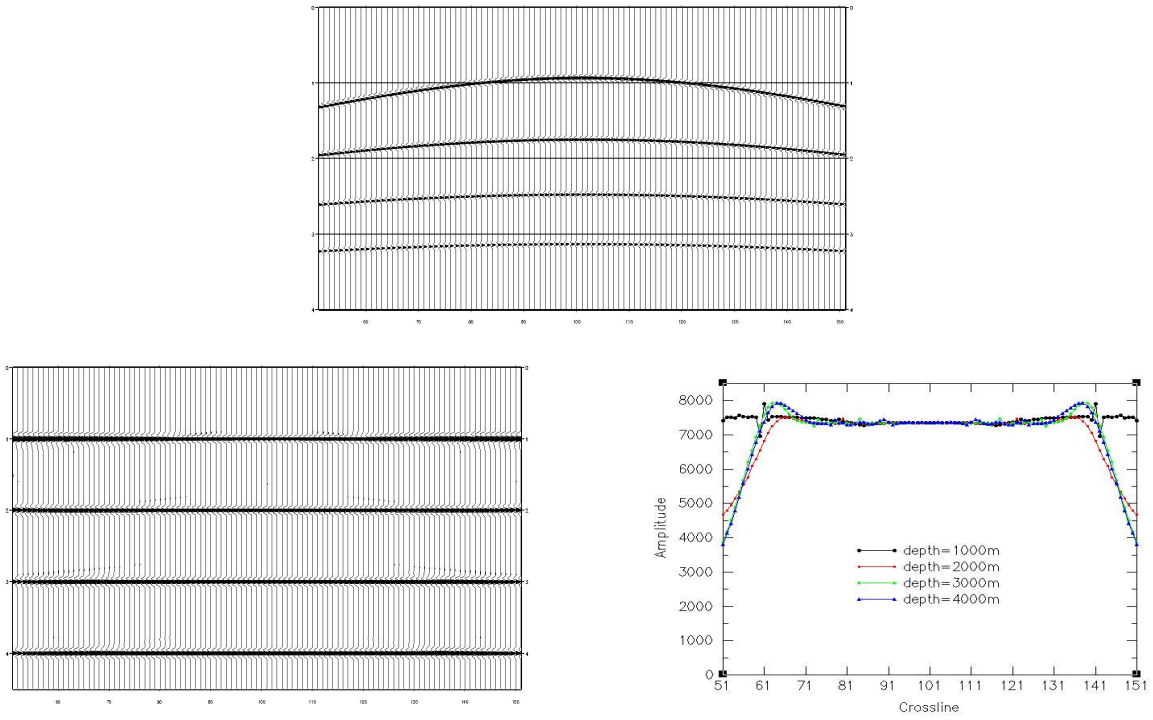

Figure 3: Top: 2-D shot record from four flat reflectors in a medium with velocity $v(z) = 2000 + 0.3z$. Bottom left: migrated shot record. Bottom right: Peak amplitudes along the migrated reflectors.